Fracture Mechanics of Concrete Structures
Proceedings FRAMCOS-3
AEDIFICATIO Publishers, D-79104 Freiburg, Germany

FAILURE BEHAVIOR OF THE RC COLUMNS WITH STEEL FIBER AS SHEAR REINFORCEMENT

S. Matsuo, S. Matsuoka, H. Yanagi and S. Doi,
Institute of Technology, Tekken Corporation, Narita, Japan

Abstract

Compared with a plain concrete member, a steel-fiber-reinforced concrete (SFRC) member is superior in cross sectional capacity and toughness, thanks to the steel fibers creating a bridging effect in the cracking cross section. In this paper, the reverse cyclic loading tests are conducted in order to grasp the influence of the mixture of steel fibers on the shear capacity and on the deformation performance. Experimental results indicate that steel fiber is effective for shear reinforcement. In addition, in order to simulate the failure behavior of an SFRC member, the non-linear finite element analysis based upon the failure mechanics has been conducted.

Key words: steel-fiber-reinforced concrete, shear capacity, non-linear finite element analysis

1 Introduction

Numerous concrete structures were disastrously damaged by the Hyogo-ken Nanbu Earthquake in 1995. In concrete structures constructed according to the conventional design standards, not a few cases of

concrete structures were reported, the cause of falling down which is attributable to the shear failure of the members. The current standards for seismic design are intended to provide the requirements for structures having a high seismic performance with an enhanced shear capacity and an improved deformation capacity. The ordinary measures for achieving this purposes involve more dense arrangement of shear reinforcement and placement of lateral ties. These measures pose, however, some problems in the construction practices such as concrete placement.

The authors et al. (1997a) have been studying, therefore, reinforced concrete components using steel fibers. In steel-fiber-reinforced concrete (SFRC), tensile stresses are transmitted in the crack surfaces due to the bridging effect of steel fibers. Consequently, SFRC components present a higher sectional capacity compared with plain concrete elements. Besides, it has been demonstrated that, since loads are borne even after the maximum sectional load is reached (improved post-peak behavior), an excellent toughness is offered. These premium characteristics of SFRC are expected to be also provided in reinforced concrete (RC) components. Such components may achieve a sufficient seismic performance even with a shear reinforcement amount equal to or less than the volume used in the conventional practices.

This paper reports the results of the reverse cyclic loading tests conducted for the purpose of obtaining knowledge on the deformation behavior of RC columns with steel fibers. Moreover, it reports the results of the fracture process simulation based on the fracture mechanics, using the non-linear finite-element analysis.

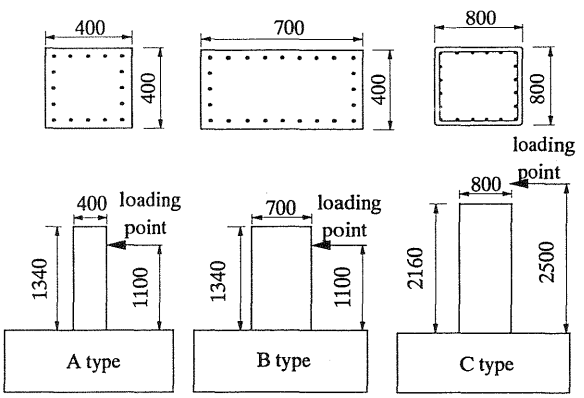

Fig. 1. Dimensions of test specimens

2 Reverse cyclic loading tests

2.1 Summary of the tests

Three types of test specimens which had a rectangular-section column (see Fig. 1) were used in the test. These specimens simulate piers of rigid frame viaduct. A type is a model of 1/2 size of the actual structure, B type has a smaller shear span ratio than A type, C type is a full scale model which simulate the pier of the Super-Express train damaged in the Hyogo-ken Nanbu Earthquake. For A and B types, no shear reinforcement is arranged while, for C type, round bars of 9mm in diameter are placed at intervals of 150mm equal to an actual structure.

The concrete mix proportions are listed in Table 1. One percent (by volume) of deformed steel fibers (indented type) 30mm long, 0.6mm in nominal diameter were added. For comparison, specimens of plain concrete were prepared for A type.

Table 1. Mix proportion of concrete

Concrete type	Unit content (kg/m^3)					
	W	C	S	G	SF	Ad
Plain	166	377	936	906	0	1.880
SFRC	176	401	1035	718	78	2.000

where; SF:steel fiber, Ad:air entraining and water reducing agent

2.2 Test procedures

In the reverse cyclic loading test, horizontal loads were applied in both positive and negative directions, under a constant compressive force. The loading equipment is outlined in Fig. 2. Three cycles of alternate loading were conducted in such a manner that displacements equal to $\delta y \times n$ (n=

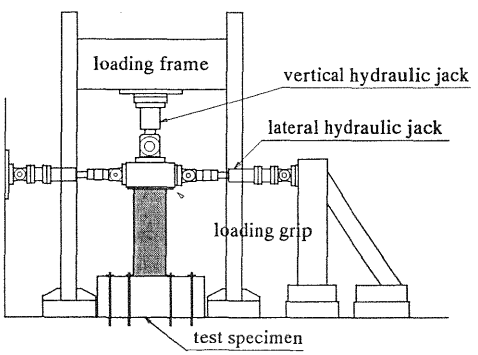

Fig. 2 Loading equipment

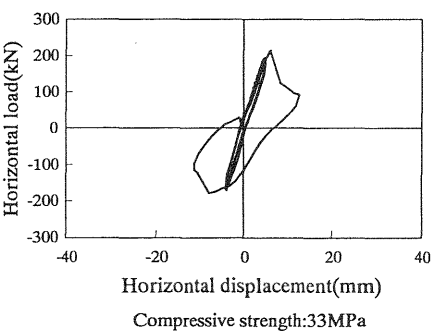

Fig. 3 Test result of A1

$\pm$1,2,3$\cdots$) may be produced successively; where δ y is the horizontal displacement of the loading point when the strain of the longitudinal reinforcement reaches the yield value. The loading was finished when the horizontal load at each stage became less than 80% of the load at the yield strain.

2.3 Test results

2.3.1 Half-scale specimens

Three half-scale specimens, A1, A2 and B were prepared. In every case an axial compressive stress of 1MPa was applied. Fig. 3 summarizes the test results for A1 specimen. Along with increasing load, diagonal cracks were initiated and propagated, resulting in shear fracture, when the strength lowered abruptly.

For A2 specimen with steel fibers, the load-displacement curve is drawn in Fig. 4. As known from this figure, the load reached its maximum when the horizontal displacement is 5 δ y, and almost no decrease in load was recorded till 8 δ y horizontal displacement was generated. After this point, the load decrease becomes more remarkable. Then, monotonous loading in the positive direction was done; even with a horizontal displacement of 65mm (limit of the hydraulic cylinder stroke), the specimen had a sufficient strength. They were observed that cracks distributed at the surface of the specimen and that steel fibers restrainted the detachment of covering.

Fig. 5 is the load-displacement curve for B specimen having a relative small shear span to depth ratio of 1.67. The general tendency is similar to the case of A2. But, the load suddenly decreases when the horizontal displacement reaches 11 δ y. At this final stage, diagonal cracks were found in the specimen. From this, it can be judged that the specimen underwent shear failure after the bending yield.

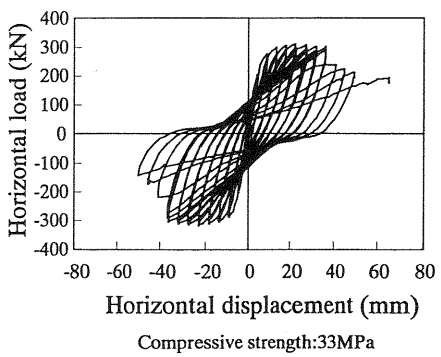

Fig. 4 Test rezult of A2

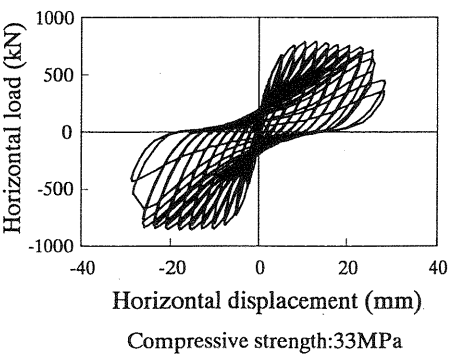

Fig. 5 Test rezult of B

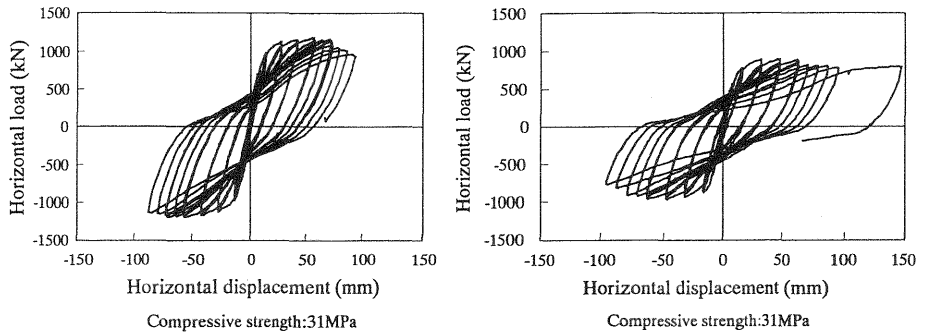

(a) C1 specimen (b) C2 specimen

Fig. 6 Test results of C type specimens

2.3.2 Full-scale specimens

The full-scale specimens were subjected to tests with different axial compressive stresses. The load-displacement curves for C1 and C2 specimens are shown in Fig. 6. The axial compressive stress is 4MPa for C1, while 1MPa for C2. Similar behaviors are found in the results of these two cases, that is, the maximum load was recorded at around a horizontal displacement of 6 δ y and the trend of post-peak load decrease is similar in the two types of specimens. But, due to the difference in axial compressive force, the maximum load in C1 is larger. Although, after a certain amount of displacement (80 to 90mm) was generated, C2 specimen experienced monotonous loading up to the limit of loading equipment stroke, a load of about 800kN was borne even with a horizontal displacement of 147mm. In terms of cracking, both C1 and C2 specimens were almost the same; the crack distribution and peeled-off concrete covering were observed.

2.3.3 Discussion on the test results

Table 2 summarizes the test results. Though, for B specimen, it finally undergoes shear failure, the ultimate point is reached after the bending yield of the longitudinal reinforcement, offering a maximum strength much higher than the calculated shear capacity. The other three specimens failed by bending failure, without experiencing shear failure. These results demonstrate the shear capacity increasing effect of mixed steel fibers. As for the rotation angle (horizontal displacement divided by height of the measured point) at the maximum displacement too, the steel-fiber mixed concrete specimens provide a significantly greater angle than the specimen without fibers. This result verifies a significant improvement effect offered by steel fiber mixture for the deformation performance.

Table 2. Experimental results

Test specimen	δ y (mm)	Load at δ y (kN)	Maximum load (kN)	Maximum displacement (mm)	Maximum rotation angle
A1	4.7	194	214	6.0	1/184
A2	4.5	202	315	65	1/17
B	2.5	463	850	27.5	1/40
C1	7.0	688	1127	91	1/23
C2	7.8	563	945	147	1/14

where; the height of the measured point is 1100mm at specimens A1, A2 and B, and 2100mm at specimens C1 and C2.

3 Simulation of fracture behavior

3.1 Purpose of the simulation

The significant effects of steel fiber mixture was experimentally confirmed for RC columns as discussed above. It should be noted, however, that the tests reported here used only one type of steel fiber and one mixture ratio. It is necessary to carry out experiments varying these parameters. But, there are a wide variety of steel fibers available in the market, and the mixing ratio varies with the application of structures. So, it is difficult to experimentally verify every case.

The authors et al. (1997b) proposed a technique for easily determining the tensile fracture characteristics (transmitted tensile strength and tension softening curve gradient) on the basis of bending test results using various steel fibers. Moreover, the authors et al. (1998) demonstrated that, by using the two parameters obtained by this method, it is possible to approximate the sectional capacity of components. On the basis of these researches, we investigated the effectiveness of evaluation method for the improvement effects of diversified steel fibers.

3.2 Finite-element analysis model

3.2.1 Tensile fracture characteristics

The tensile fracture characteristics of steel-fiber-reinforced concrete are usually expressed by a tension softening relationship which is a bilinear model. Nanakorn (1993) verified its second straight line alone is sufficient in practical design. This linear model is determined by the transmitted tensile stress through the steel fibers and the gradient of the tension softening curve. In the present analysis, a tension softening curve, which is the linear model in Fig. 7, was constructed on the basis of 4-

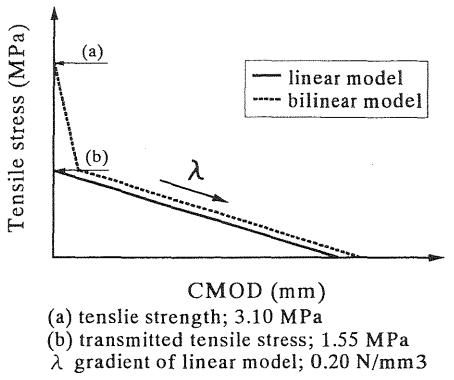

(a) tenslie strength; 3.10 MPa
(b) transmitted tensile stress; 1.55 MPa
λ gradient of linear model; 0.20 N/mm3

Fig. 7 Tension softening model

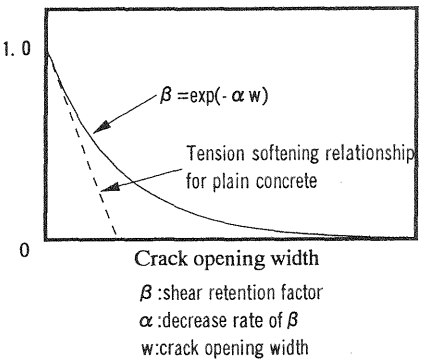

β :shear retention factor
α :decrease rate of β
w:crack opening width

Fig. 8 Shear retention factor

points bending test results of steel fiber reinforced concrete having the same properties as that used in the reverse cyclic loading test.

3.2.2 Stress-strain relationship

The compressive stress-strain relationship of concrete is expressed by a quadratic type curve according to "Standard Specification for Design and Construction of Concrete Structures" by JSCE. But, the limit strain was fixed as 3.5% from the results of the simulation of 40cm square section members, which was implemented separately. The Drucker-Prager type yield surface was used. The tensile stress-strain relationship of concrete before crack occurs is assumed to be expressed by the elastic modulus equal to the gradient of the tangent to the compressive stress-strain curve at the origin.

The reinforcing bars are supposed to follow a perfect elasto-plastic curve. The bars were modeled by truss elements solely bearing axial forces. The nodes were common with those of the rectangular elements used for modeling the concrete.

3.2.3 Shear retention factor of cracked elements

The shear stiffness of cracked elements is assumed to depend upon the crack opening width in the smeared crack model, the opening being the displacement in the major principal stress direction minus the elastic deformation. "Shear retention factor" which is the dimensionless expression of the shear stiffness of the cracked elements in terms of the shear stiffness before cracking. The decrease rate of shear retention factor α is determined, as shown in Fig. 8, in such a manner that the tangent gradient of the shear retention factor immediately after crack initiation equal to the gradient of the tension softening curve made dimensionless in terms of tensile strength.

3.2.4 Numerical model

The numerical research involved rectangular isoparametric elements under two-dimensional stresses. It is assumed in the analysis that, when the major principal stress reaches the tensile strength magnitude of the concrete, a crack occurs in the direction normal to the major principal stress. The deformation in the direction normal to the crack face in the cracked elements is considered in modeling to be a sum of the crack opening width and the elastic deformation other than the crack. The tensile stress-strain relationship in the major principal stress direction can be expressed by the tension softening curve and stress-strain relationship in the elastic region other than the cracked elements. When converting the tension softening curve into the stress-strain relationship, the concept of "equivalent length" (Dahlblom et al. 1990) was resorted to for avoiding the dependency upon the element size. The stress-strain relationship in the minor principal stress is that before cracking. Besides, for the purpose of considering the crack localization in brittle materials, we judged whether or not the tensile characteristics of the cracked element branches to the unloading path.

3.3 Analytical results

The results of numerical study on the reverse cyclic loading tests are given in Fig. 9 through 11. In each figure, the envelope curve in the positive directio is used in order to express the experimental result. Though reverse cyclic loading was done in the experiments, the analysis used monotonous loading. The curves in Fig. 9 are the analytical and experimental results of A2 specimen. The numerically obtained yield load is almost the same as the experimental result. The maximum load is, however, greater in the experiments. This can be explained as follows; the load does not increase after the longitudinal reinforcing-bar yield in the analysis, since the stress-strain relationship of the re-bars is assumed to be

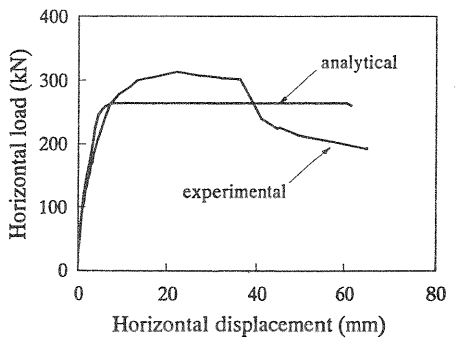

Fig. 9 Analytical result of A2

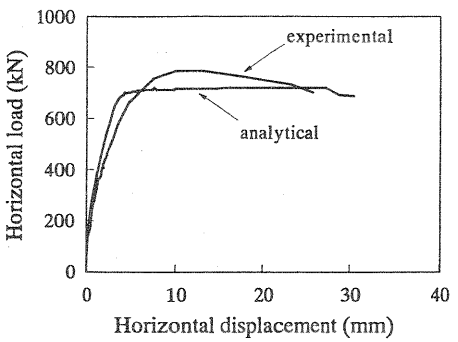

Fig. 10 Analytical result of B

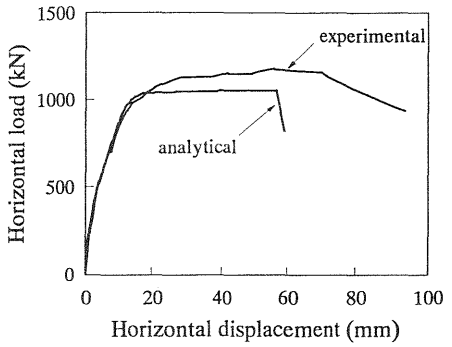

Fig. 11 Analytical result of test specimen C1

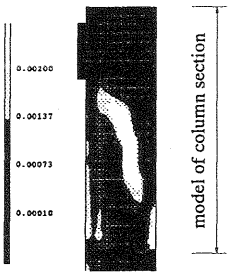

(Each value indicates the strain per equivalent length.)

Fig. 12 Appearance of crack distribution for A1

perfect by elast-plastic; but, the actual relationship is not perfect so. Experimentally, a load decrease is observed with a horizontal displacement of about 35mm, whereas, analytically the load is borne up to 60mm. The experiments used alternate loading, with 3 repetitive load applications for each magnitude of displacement. In contrast, the analysis involved monotonous loading in the positive direction alone. Consequently, the energy loss may be smaller in the analysis.

Fig. 10 illustrates the analytical result of B specimen. Looking at the loads, the same tendency is found as A2 specimen. For horizontal displacements, there is almost entire agreement between experimental and analytical results. As for the result of C1 specimen shown in Fig. 11, the analytical ultimate displacement is smaller than the experimental results. This may be attributable to the component size, because the limit compressive strain used in the analysis was determined from the results of 40cm square members tests. Fig. 12 shows the appearance of crack distribution of A2 specimen. The analytical result, like the experimental result, provide a representative pattern of steel-fiber-reinforced concrete.

As discussed above, the analysis expresses with a satisfactory accuracy the general trend of load-displacement curves and cracking behavior. It can be said that simulation is effective qualitatively. Therefore, effective analysis is possible also for cases with various steel fibers. By comparison between analytical results of different steel fibers, we can judge the degree of reinforcing effectiveness dependent upon the steel fiber types. It should be noted, however, that there is some difference in maximum load and ultimate horizontal displacement between analytical and experimental results. For improving such a drawback, it is essential to improve the modeling accuracy of stress-strain curves of concrete and reingforcing bars. Moreover, it is necessary to correctly evaluate the unloading and reloading paths. Three-dimensional analysis may be required, for expressing the confining effect of concrete, etc.

4 Summary

The knowledge obtained through the study is summarized as follows.

1. Mixture of steel fibers provides an additional shear capacity. It transform a shear-failure type RC column into a bending-failure type.
2. In RC columns using steel fibers, the rotation angle at the maximum displacement is greater compared with an RC column, that is to say, the deformation performance is enhanced.
3. The two dimensional finite-element analysis based on the fracture mechanics is capable of qualitatively simulating reverse cyclic loading tests. By this analysis, we can judge the degree of reinforcing effect dependent upon the nature of steel fibers.
4. For simulation of higher accuracy, we should revise the analytical model and implement three-dimensional analysis.

5. References

Dahlblom, O. and Ottosen, N.S. (1990) Smeared crack analysis using generalized fictitious crack model. **Journal of Engineering Mechanics.**, Vol.116, No.1, 55-76.

Masuda, A., Matsuoka, S., Matsuo, S. and Takeda, Y. (1997a) Static alternating cyclic loading tests of steel fiber reinforced concrete columns (in Japanase), in **Proceedings of the Japan Concrete Institute**, Vol.19, No.2, Tokyo, 1521-1526.

Matsuoka, S., Matsuo, S., Masuda, A. and Yanagi, H. (1997b) A test method for tensile property of steel-fiber-reinforced concrete (in Japanese). **J. Materials Conc. Struct., Pavements**, JSCE, No.564/V-35, 297-316.

Matsuoka, S., Masuda, A., Matsuo, S. and Yanagi, H. (1998) A study on simulation of tunnel lining with steel-fiber-reinforced concrete (in Japanese), **J. Materials Conc. Struct., Pavements**, JSCE (will be pulished).

Nanakorn, P. (1993) **Fracture Mechanics based Design Method of SFRC Tunnel Lining.** Doctoral Thesis of Department of Civil Engineering, The University of Tokyo, Tokyo.